62 10012 Copy 527

[redacted] NASA TM X-648

NASA TM X-648

TECHNICAL MEMORANDUM

X – 648

SOME EFFECTS OF FLARE AND NOSE SHAPE ON THE DAMPING-IN-PITCH CHARACTERISTICS OF A BLUNT-NOSED FLARE-STABILIZED BODY AT TRANSONIC MACH NUMBERS

By James C. Monfort and Phillips J. Tunnell

Ames Research Center
Moffett Field, Calif.

N70-78444
(ACCESSION NUMBER) (THRU)
25 (PAGES) (CODE)
(NASA CR OR TMX OR AD NUMBER) (CATEGORY)
FACILITY FORM 602

CLASSIFICATION CHANGED
UNCLASSIFIED
To
By authority of NASA TD 10408 Date 12/23/70

[redacted]

Declassified by authority of NASA
Classification Change Notices No. 210
Dated **12-15-70

[redacted]

NATIONAL AERONAUTICS AND SPACE ADMINISTRATION

WASHINGTON [redacted] February 1962

[redacted]

CONFIDENTIAL

1Y

[redacted]

NATIONAL AERONAUTICS AND SPACE ADMINISTRATION

TECHNICAL MEMORANDUM X-648

SOME EFFECTS OF FLARE AND NOSE SHAPE ON THE DAMPING-IN-PITCH CHARACTERISTICS OF A BLUNT-NOSED FLARE-STABILIZED BODY AT TRANSONIC MACH NUMBERS*

By James C. Monfort and Phillips J. Tunnell

SUMMARY

The results of an experimental wind-tunnel investigation to measure the static force and moment coefficients and the damping-in-pitch coefficients of a blunt-nosed flare-stabilized re-entry vehicle are presented.

Three flare shapes were investigated in combination with a blunted conical nose and a 2:1 fineness ratio ellipsoidal nose on an essentially cylindrical forebody. Data were obtained over a range of Mach numbers from 0.70 to 1.35 corresponding to a Reynolds number per foot of 5 to 8.5 million.

A strong influence of flare shape on the dynamic characteristics was observed for this vehicle. It was found that at certain Mach numbers the damping moments became destabilizing at lower angles of attack as the flare angle was increased.

INTRODUCTION

The advantages of a blunt nose for a re-entry vehicle in the hypersonic speed range are well known. However, recent wind-tunnel and free-flight investigations have demonstrated some stability problems for blunt-nosed vehicles in the transonic speed range. These problems are manifested as strongly nonlinear pitching moments and destabilizing damping moments which are associated with the separation of the flow about the vehicle (ref. 1). Free-flight tests reported in reference 2 indicated a limit-cycle type of oscillation of the order of $\pm 25^{\circ}$ for a blunt-nosed body. A study of flow separation on such bodies was reported in reference 3.

[redacted] Unclassified

[redacted]

The present investigation was undertaken originally to assess the aerodynamic effects of the changes in model contour due to ablation of the re-entry stage of a ballistic missile. The scope of the investigation was later broadened to include various combinations of nose and flare shapes in an effort to ascertain the relative importance of these geometric parameters at Mach numbers from 0.70 to 1.35 on static and dynamic characteristics.

NOTATION

C_A	axial-force coefficient, $\frac{\text{axial force}}{(1/2)\rho V^2 S}$
C_m	pitching-moment coefficient, $\frac{\text{pitching moment}}{(1/2)\rho V^2 S d}$
$C_{m_q} + C_{m_{\dot{\alpha}}}$	damping-in-pitch coefficient, $\frac{\partial C_m}{\partial(qd/V)} + \frac{\partial C_m}{\partial(\dot{\alpha}d/V)}$, per radian
C_N	normal-force coefficient, $\frac{\text{normal force}}{(1/2)\rho V^2 S}$
d	diameter of base of nominal 9°-17° flare, 1.256 ft
f	frequency of oscillation, cps
l	over-all body length, ft
M_∞	free-stream Mach number
q	pitching velocity, radians/sec
R	Reynolds number, based on d
S	cross-sectional area of base of nominal 9°-17° flare, sq ft
V	free-stream velocity, ft/sec
α	angle of attack, deg
$\dot{\alpha}$	$\frac{d\alpha}{dt}$, radians/sec
α_o	oscillation amplitude, deg
ρ	free-stream density, slugs/ft^3

APPARATUS

Wind Tunnel and Instrumentation

The tests were conducted in the 11- by 11-foot transonic test section of the Ames Unitary Plan Wind Tunnel, which is of the closed-circuit, variable-pressure type. A complete description of this facility is given in reference 4. In figure 1 is shown a sectional view of the 11- by 11-foot test section. In this facility the Mach number can be varied continuously from 0.60 to 1.40 at stagnation pressures ranging from 2 to 35 psia.

A
5
2
5

The static forces and moments on the models were measured by means of a sting-mounted strain-gage balance. Dynamic moments were measured by means of a forced-oscillation balance identical to the one described in reference 5. A photograph of a typical installation is shown in figure 2.

Models

A sketch of the three nose and flare shapes which were tested on a common essentially cylindrical body is shown in figure 3. The three nose shapes, in order of increasing bluntness, were a 2:1 fineness ratio ellipsoid, a 24° blunted cone representing the unablated nose, and a 26° blunted cone representing the ablated nose, the three flare shapes are designated as a nominal 10°, a nominal 9°-17° representing the ablated flare, and a nominal 10°-24° representing the unablated flare (see fig. 3). Angular values of noses and flares are referred to throughout the text by the nominal values above for convenience, with exact values shown in figure 3. For both the static and dynamic tests the same moment reference was used, the location of which is indicated in figure 3. A smooth surface condition existed for all models.

TESTS

Static Force Tests

Axial-force, normal-force, and pitching-moment coefficients were determined at angles of attack from -6° to about 15° for Mach numbers from 0.70 to 1.35. The data were not corrected for base pressure. The test Reynolds number varied within the limits shown in figure 4.

Damping-in-Pitch Tests

Dynamic stability was measured at $\pm 1^{\circ}$ pitch amplitude and at the natural frequency of the oscillatory system. The variation of the natural frequency with Mach numbers at $\alpha = 0^{\circ}$ is shown in figure 5. The Mach number and Reynolds number ranges were the same as for the static force tests. The maximum angle of attack was limited by the pitching-moment capacity of the balance.

RESULTS AND DISCUSSION

A
5
2
5

Static Force and Moment Characteristics

Typical variations with angle of attack of static axial-force, normal-force, and pitching-moment coefficients of the 26° nose in combination with the 9°-17° flare are shown in figures 6, 7, and 8, respectively. The adverse stability characteristics associated with blunt bodies at transonic speeds (ref. 1) are readily discernible in the nonlinear normal-force and pitching-moment curves at subsonic and low supersonic Mach numbers. Also shown for comparison are static pitching-moment coefficients from tests of the ellipsoidal nose in combination with the 9°-17° flare. The data for the ellipsoidal nose show none of the subsonic nonlinear moment characteristics at or near zero angle of attack that are so in evidence in data for the blunter nose. However, a nonlinearity is evident in the moment characteristics at angle of attack at a Mach number of 1.0, which for the blunt-nosed model occurs at Mach numbers from 1.0 through 1.05.

The large hysteresis loops in the pitching-moment and normal-force characteristics observed for blunter bodies in reference 1 are absent from the data of the present investigation.

Damping-in-Pitch Characteristics

The variation of damping in pitch with angle of attack is shown in figures 9 and 10 for the ellipsoidal- and conical-nosed models in combination with the three flares. The curves show regions of dynamic instability although the static pitching-moment data of this investigation do not contain hysteresis loops. However, schlieren motion pictures of the flow indicate the existence of some hysteresis under dynamic conditions. A typical set of sequential schlieren pictures taken at 64 frames per second is presented in figure 11. The oscillatory motion was about an angle of attack where a discontinuity existed in the static characteristics. Pictures (1) and (2) represent the near minimum and maximum

DECLASSIFIED

angles of attack, respectively, and the flow is attached. The flow has separated in picture (3) and remains separated with decreasing angle of attack to near the minimum, as observed in picture (4), thus forming a hysteresis loop in the one cycle shown.

Effect of Flare Shape

A 525

A large influence of flare on the dynamic characteristics is shown in figure 10. Comparison of the 10°-24° and 10° flare data indicates that the former causes the flow to separate at a lower angle of attack for a given Mach number and to remain separated over a wider Mach number range. Also the magnitudes of the unstable damping moments observed for the 10°-24° flare are, for the most part, approximately two or three times the values noted for the 10° flare. The adverse stability effects of the blunter nose of the ablated configuration, as compared to the unablated configuration, are more than offset by the beneficial effects of the reduced flare. The net result is a marked improvement in the dynamic characteristics of the blunter nosed model.

It can be concluded that both the flare and the nose shape have important effects on the dynamic characteristics for this family of vehicles in the transonic Mach number range. However, for Mach numbers of 0.95 and below the flare appears to be of less importance than the nose.

Effect of Nose Shape

Comparisons of the pitching- and damping-moment coefficients for the ellipsoidal- and blunted conical-nosed models are presented in figures 8 and 9. Nonlinear pitching moments and large unstable damping coefficients are noted for the blunted conical-nosed models over a wide Mach number range (0.70 to 1.05). The ellipsoidal-nosed model is comparatively free of these adverse characteristics. The results support the conclusions of references 1, 3, and 6 in demonstrating improved stability characteristics with decreasing nose bluntness.

Ames Research Center
National Aeronautics and Space Administration
Moffett Field, Calif., Nov. 21, 1961

REFERENCES

1. Reese, David E., Jr., and Wehrend, William R., Jr.: An Investigation of the Static and Dynamic Aerodynamic Characteristics of a Series of Blunt-Nosed Cylinder-Flare Models at Mach Numbers From 0.65 to 2.20. NASA TM X-110, 1960.

2. Mayhue, Robert J.: Free-Flight Measurements of the Base Pressures and Drag of a Flare-Stabilized Cylindrical Reentry Body With an Elliptical Blunt Nose at Mach Numbers From 1.9 to 0.7. NASA TM X-309, 1960.

3. Cleary, Joseph W.: The Effects of Nose Bluntness on the Flow Separation and Longitudinal Characteristics of Ellipsoidal-Nosed Cylinder-Flare Models at Transonic Speeds. NASA TM X-370, 1960.

4. Hunton, Lynn W.: Effects of Fixing Transition on the Transonic Aerodynamic Characteristics of a Wing-Body Configuration at Reynolds Numbers from 2.4 to 12 Million. NACA TN 4279, 1958.

5. Emerson, Horace F., and Robinson, Robert C.: Experimental Wind-Tunnel Investigation of the Transonic Damping-in-Pitch Characteristics of Two Wing-Body Combinations. NASA MEMO 11-30-58A, 1958.

6. Emerson, Horace F., and Robinson, Robert C.: The Transonic Damping in Pitch of Three Cylinder-Flare Models With Various Degrees of Nose Bluntness. NASA TM X-368, 1960.

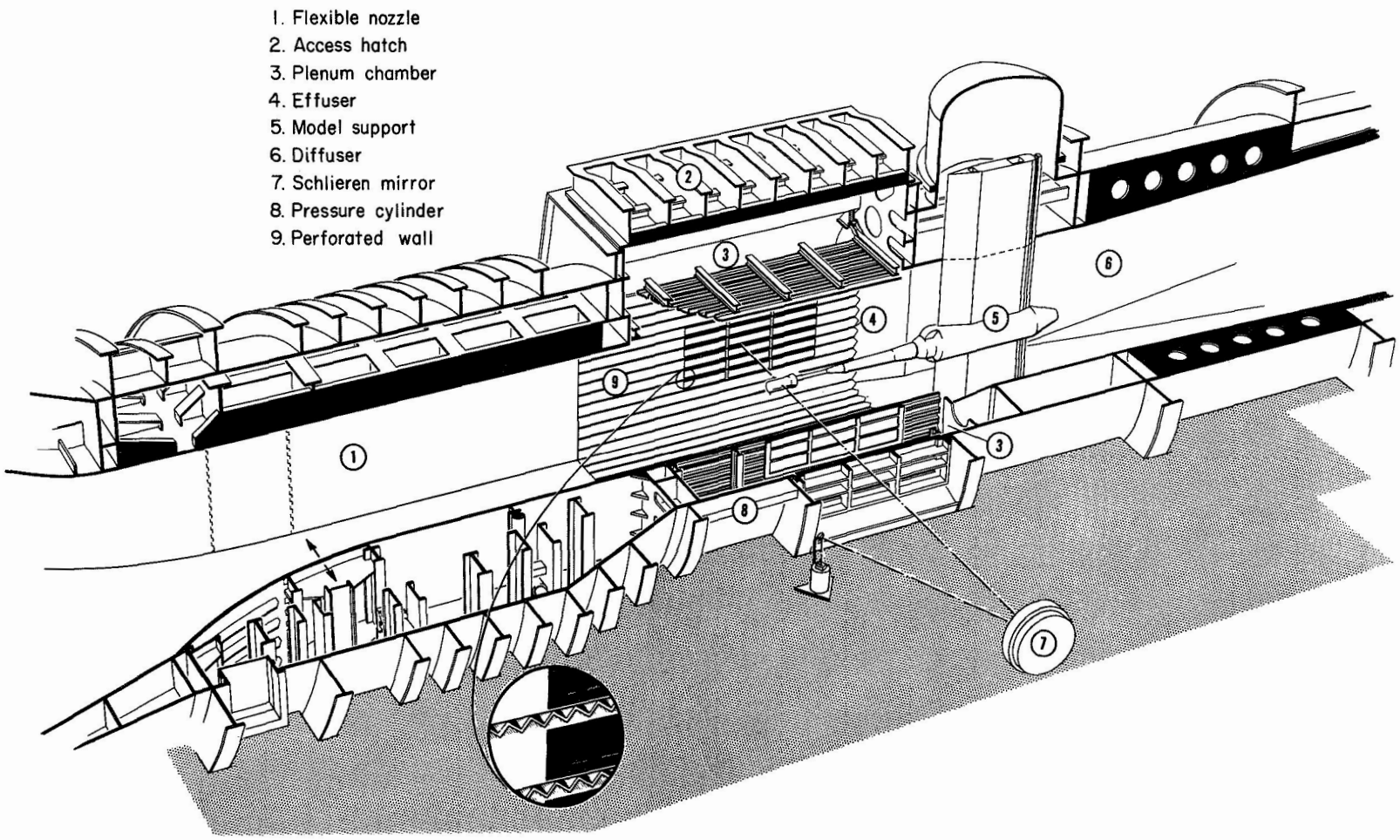

Figure 1.- Arrangement of the 11- by 11-foot test section.

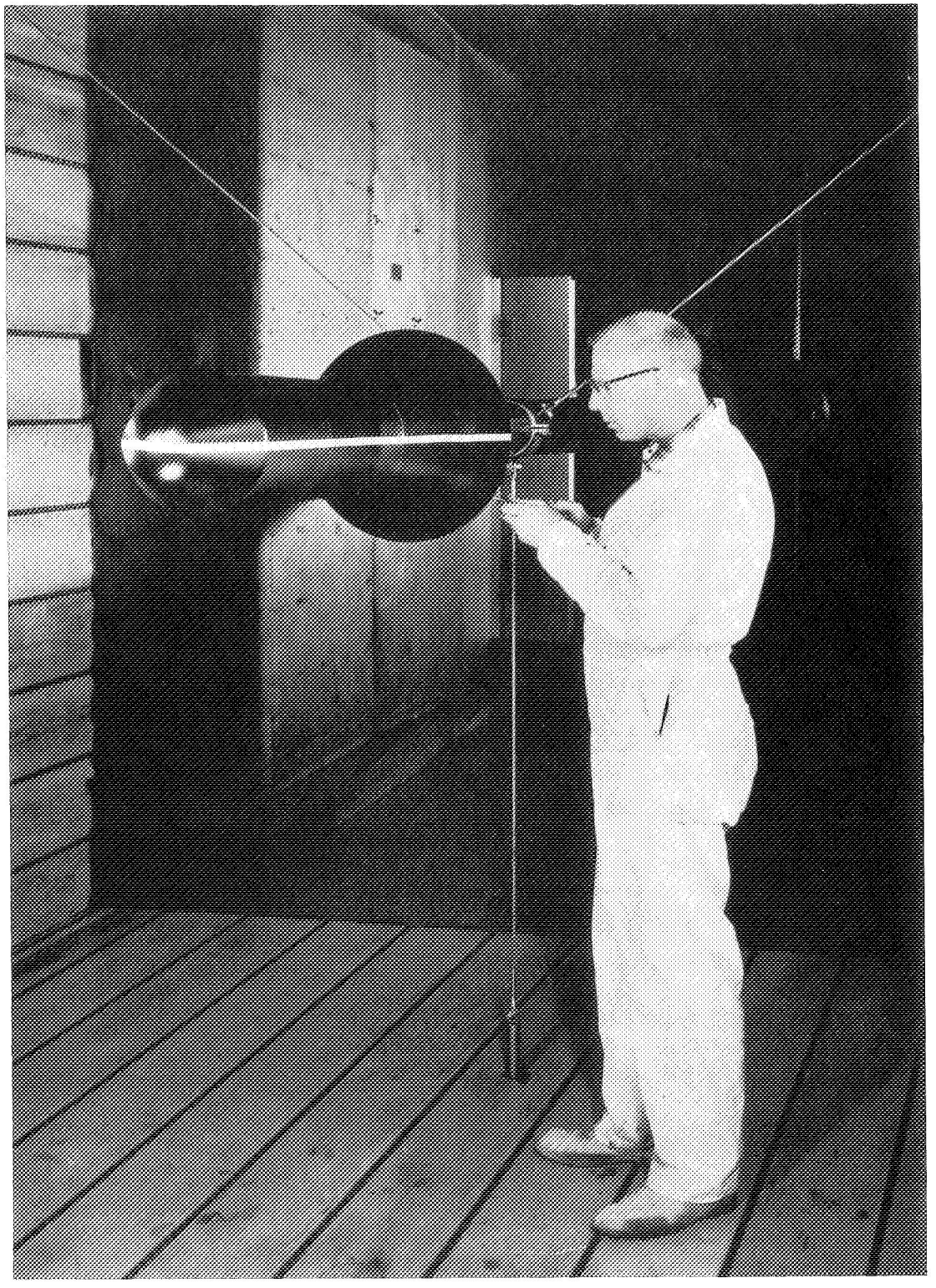

A-26423

Figure 2.- Typical model installation in the 11- by 11-foot test section.

A
5
2
5

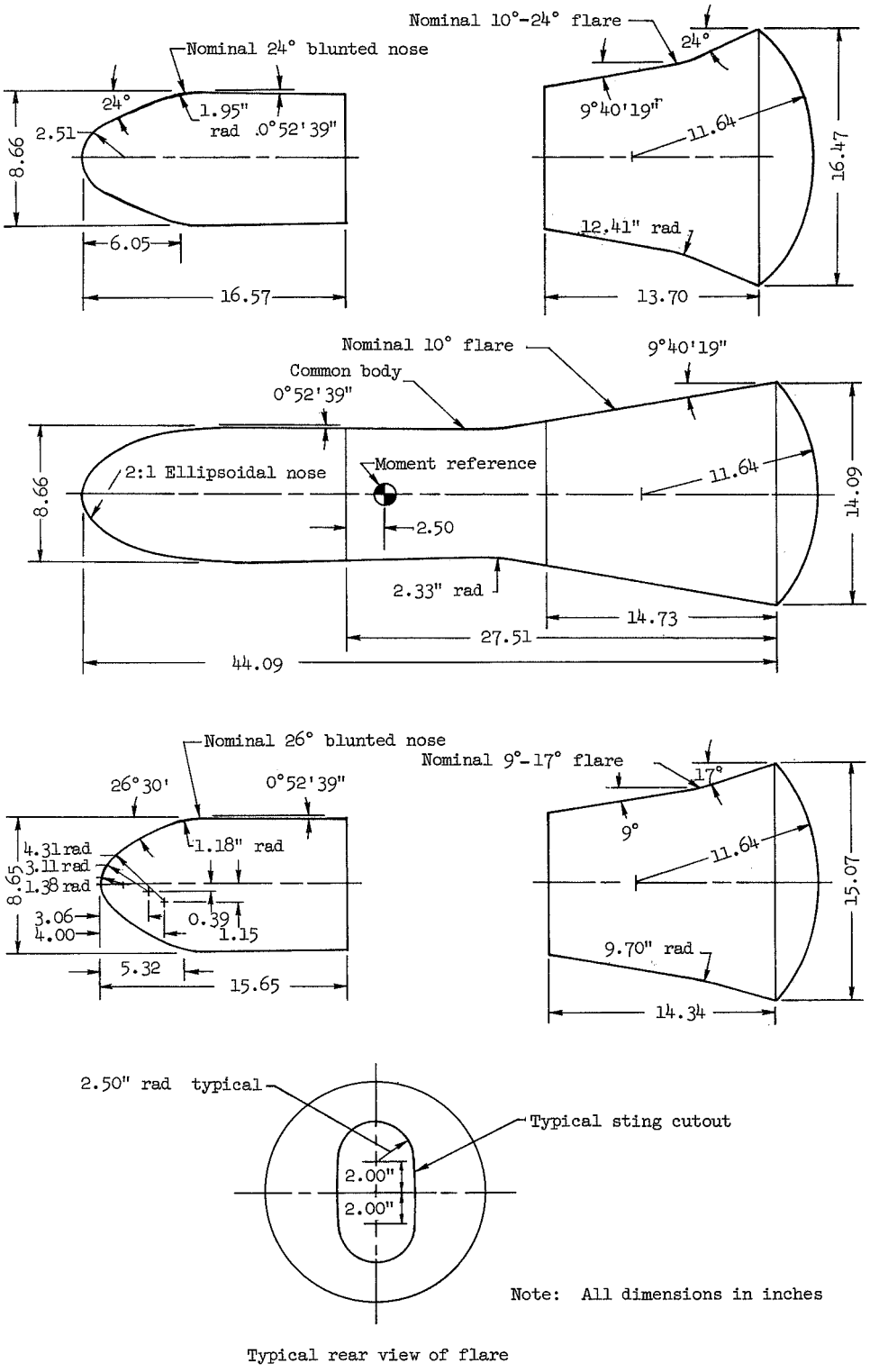

Figure 3.- Sketch of the various model components.

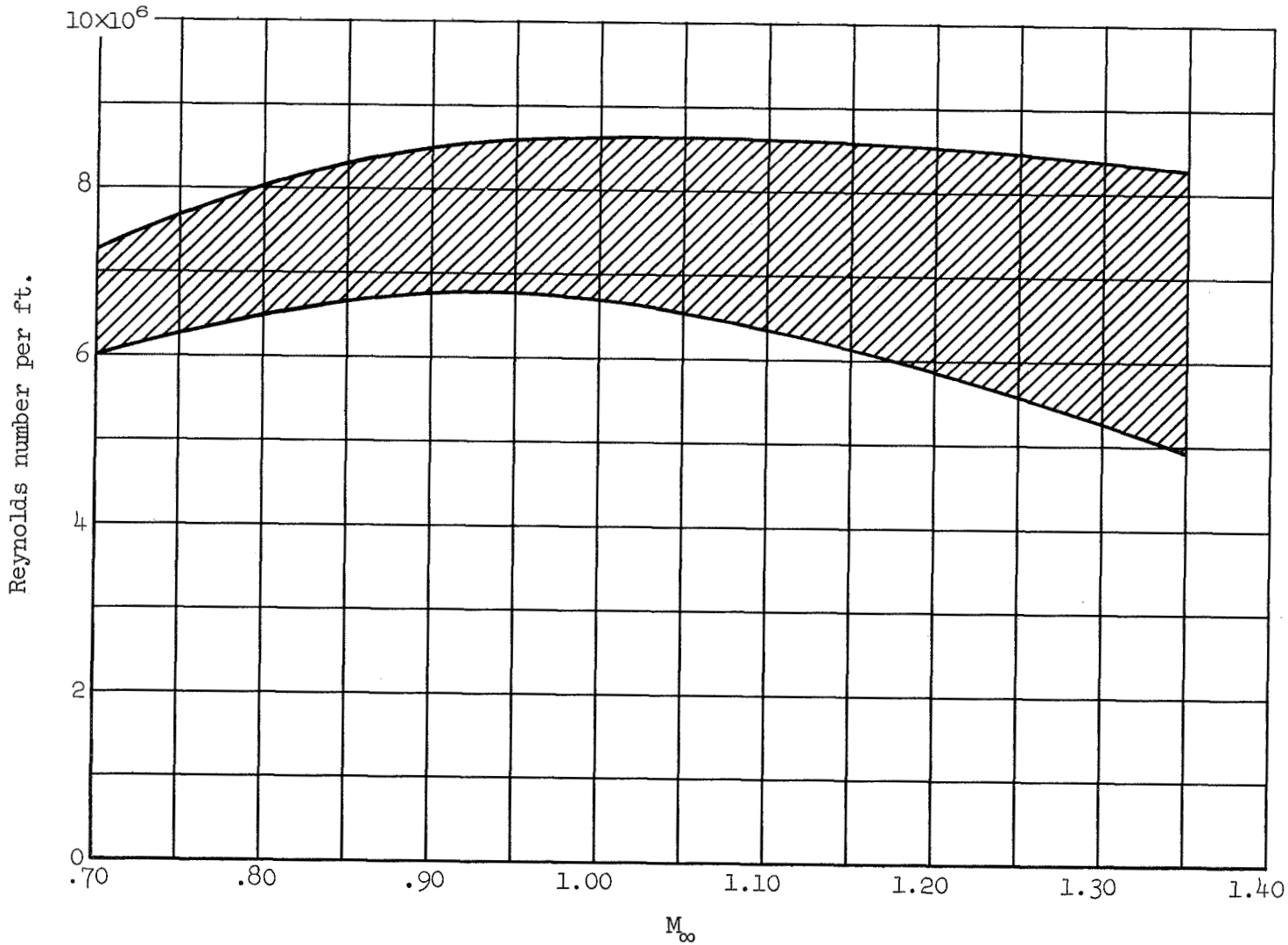

Figure 4.- Variation of Reynolds number with Mach number.

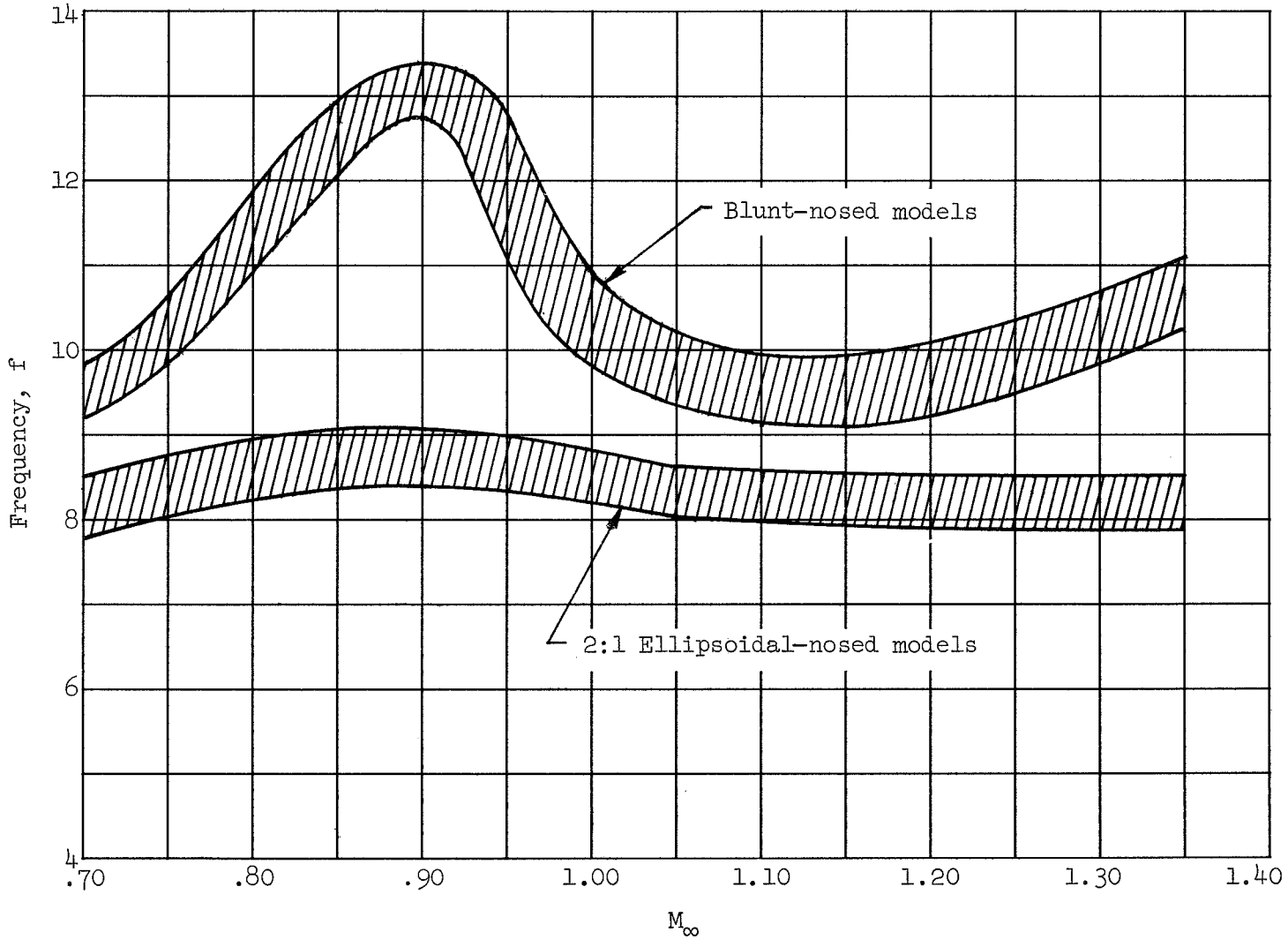

Figure 5.- Variation of frequency with Mach number.

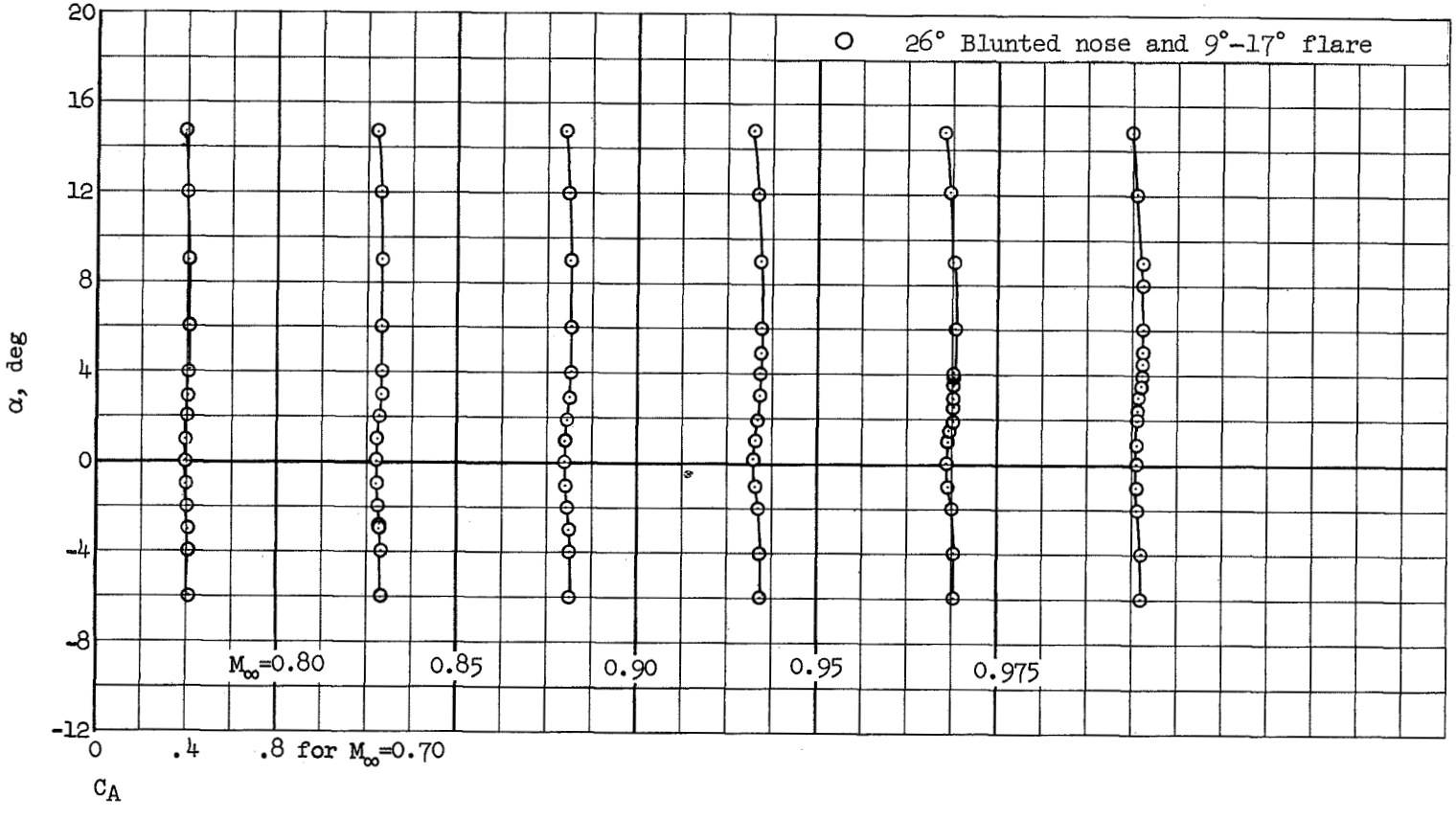

(a) M_∞ = 0.70 to 0.975

Figure 6.- Typical variation of axial-force coefficient with angle of attack at constant Mach number.

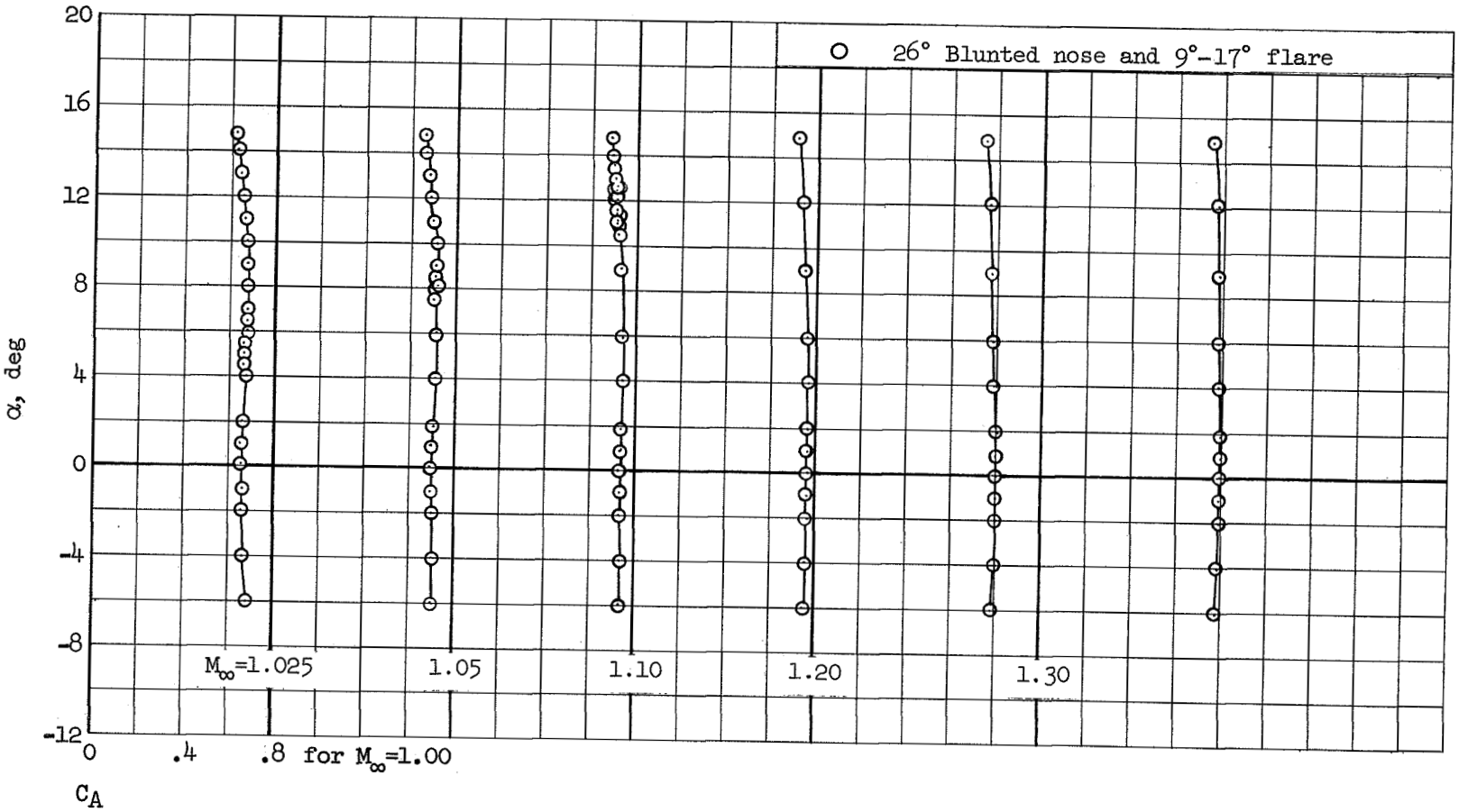

(b) M_∞ = 1.00 to 1.30

Figure 6.- Concluded.

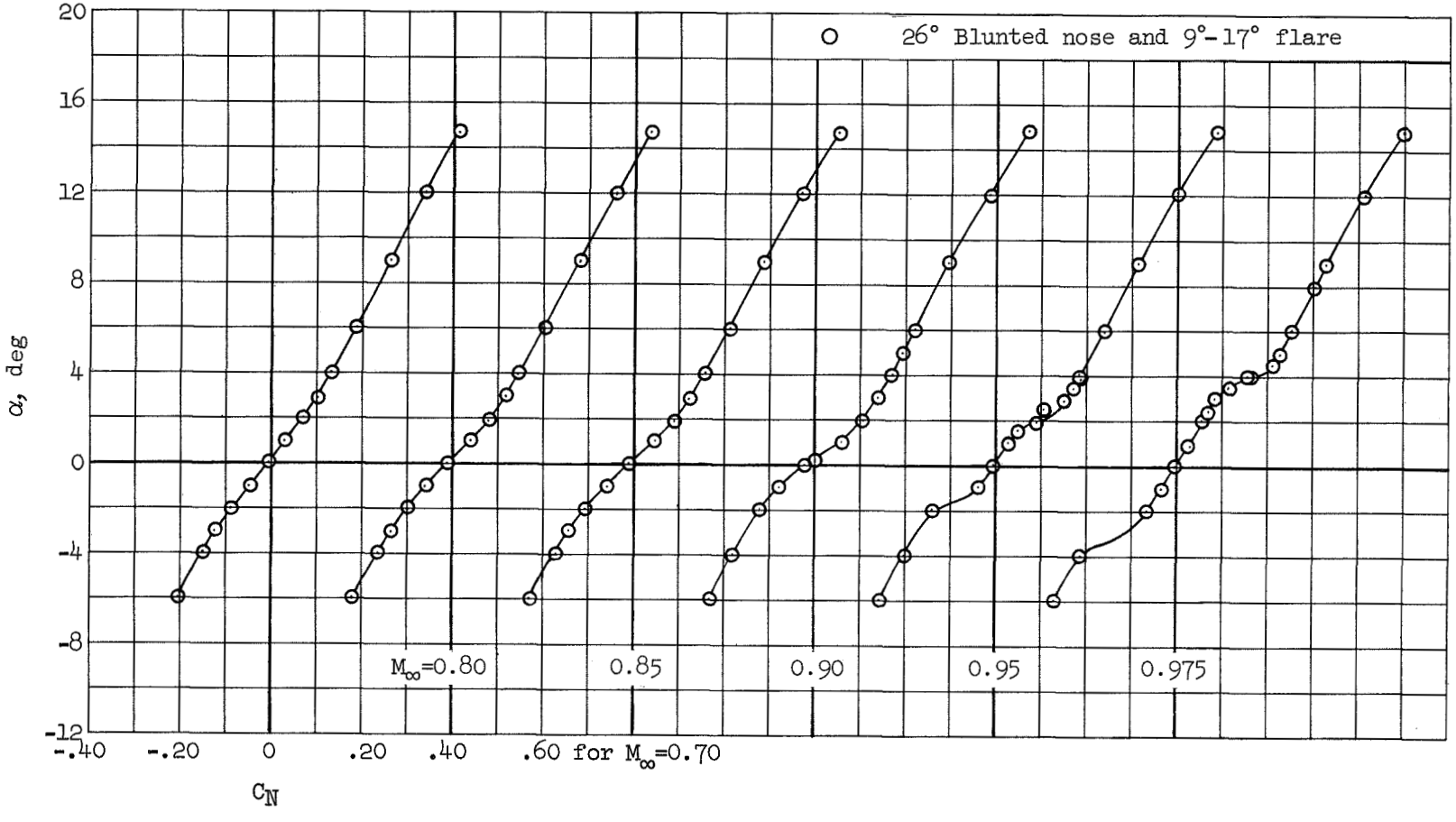

(a) M_∞ = 0.70 to 0.975

Figure 7.- Typical variation of normal-force coefficient with angle of attack at constant Mach number.

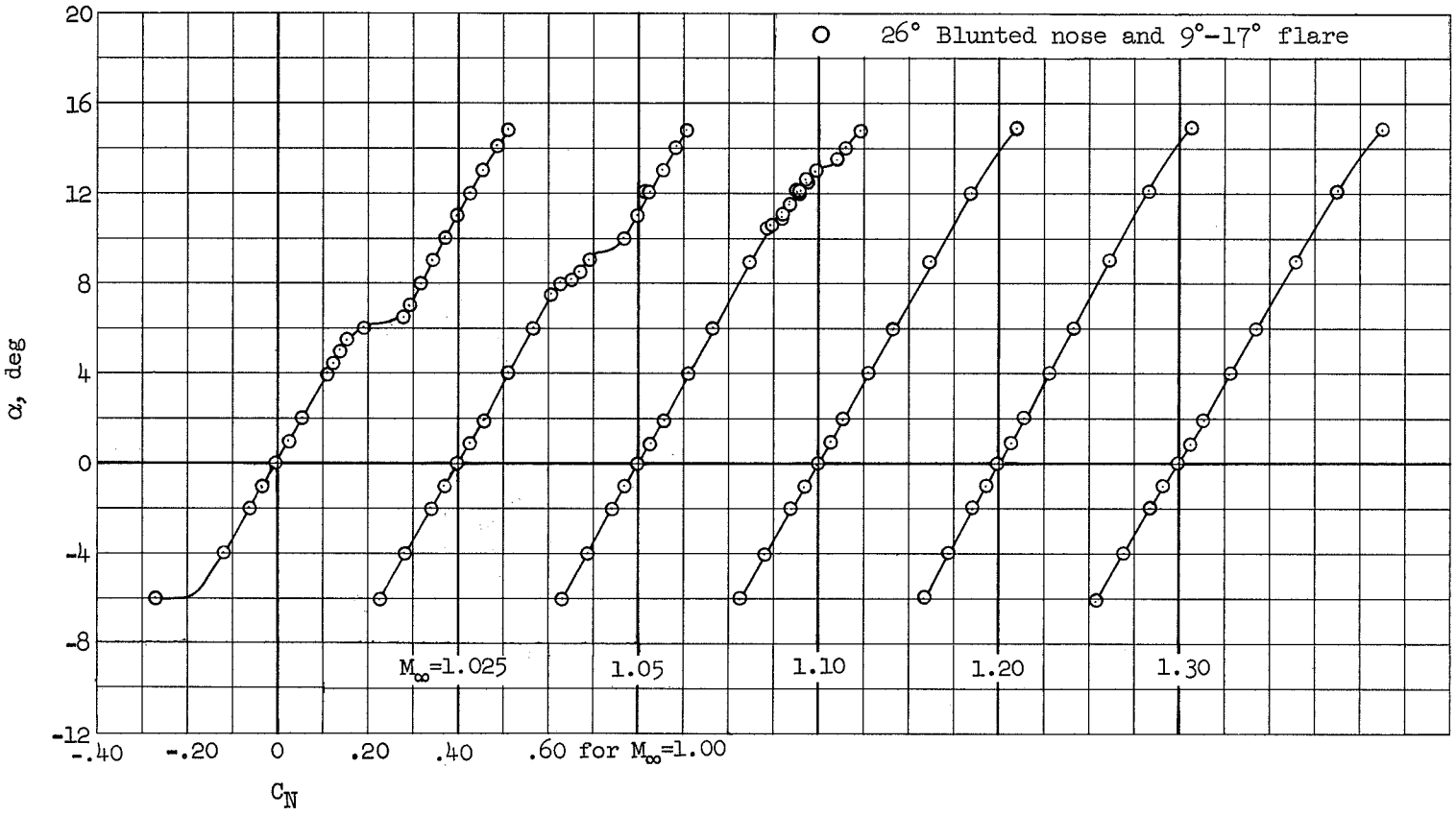

(b) M_∞ = 1.00 to 1.30

Figure 7.- Concluded.

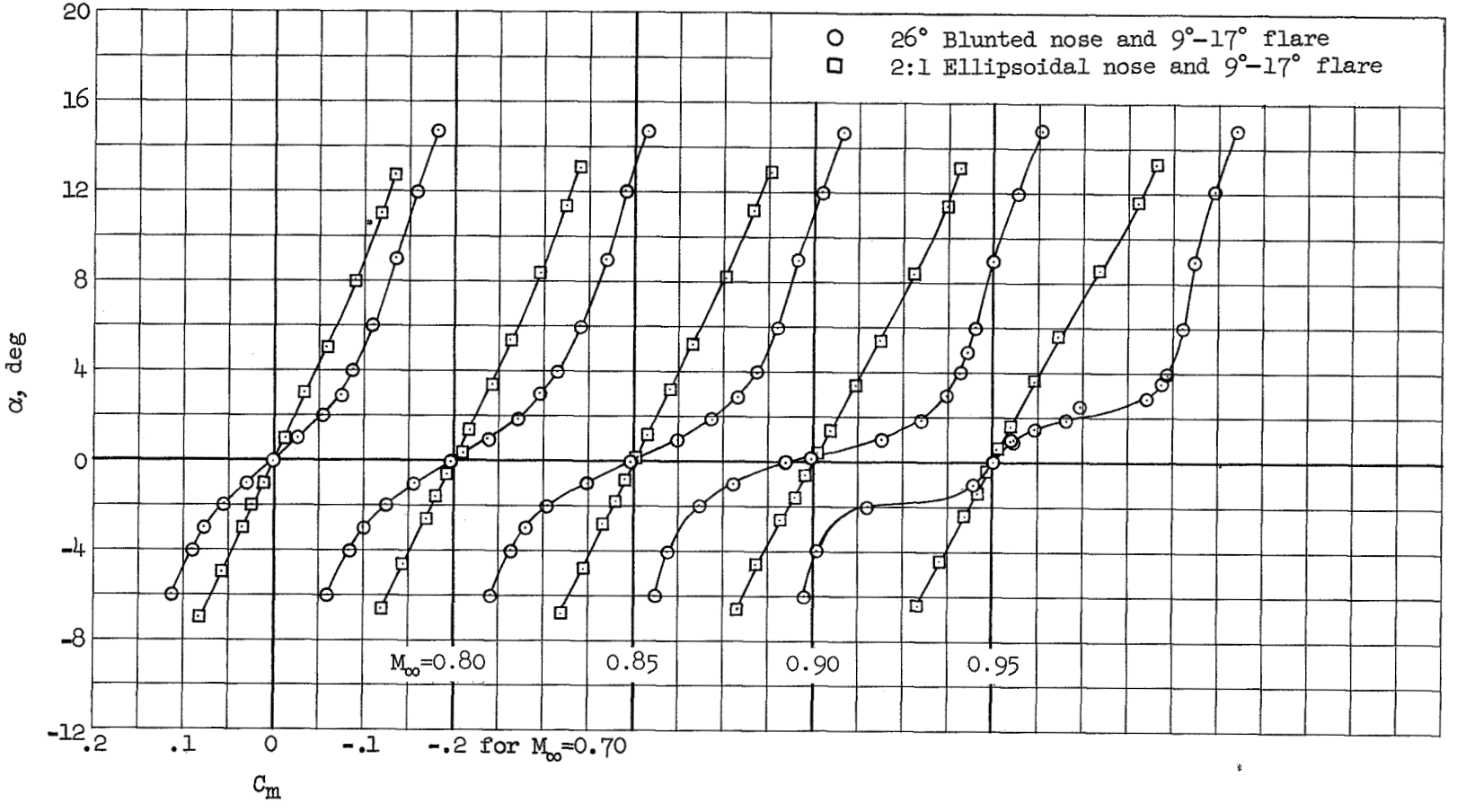

(a) M_∞ = 0.70 to 0.95

Figure 8.- Typical variation of pitching-moment coefficient with angle of attack at constant Mach number.

5254

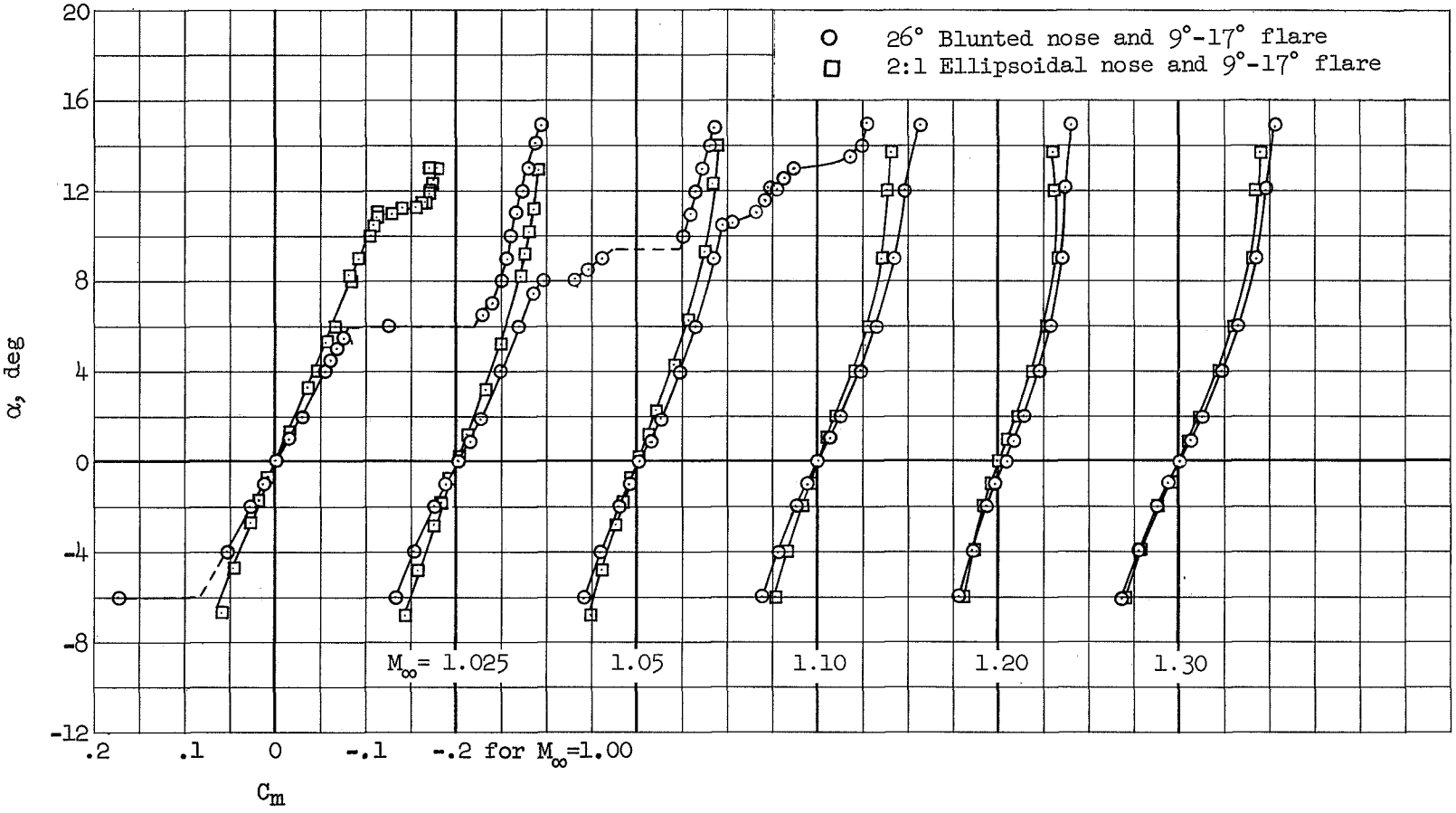

(b) M_∞ = 1.00 to 1.30

Figure 8.- Concluded.

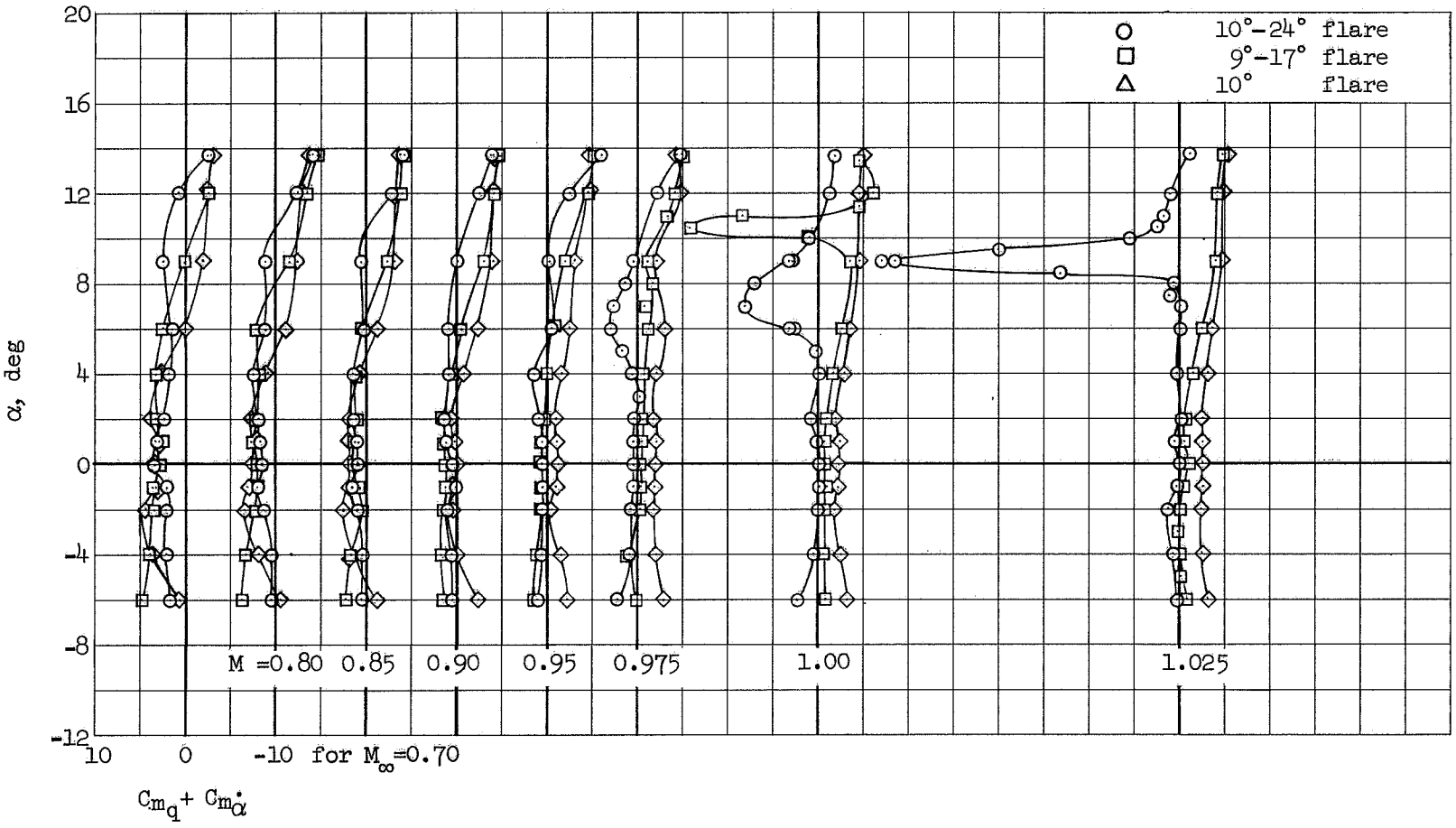

(a) M_∞ = 0.70 to 1.025

Figure 9.- Variation of the damping in pitch with angle of attack at constant Mach number for ellipsoidal-nosed models.

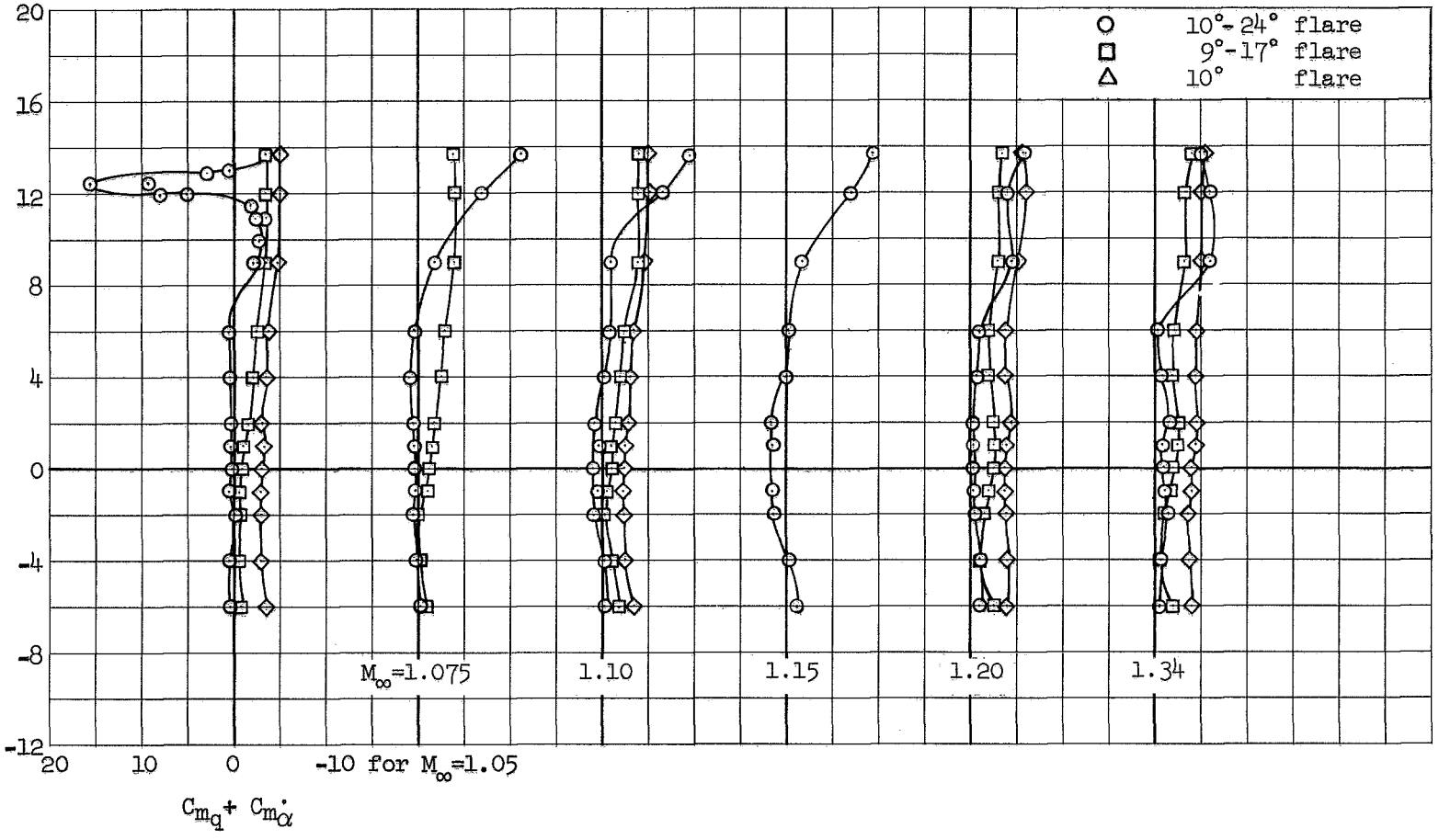

(b) M_∞ = 1.05 to 1.34

Figure 9.- Concluded.

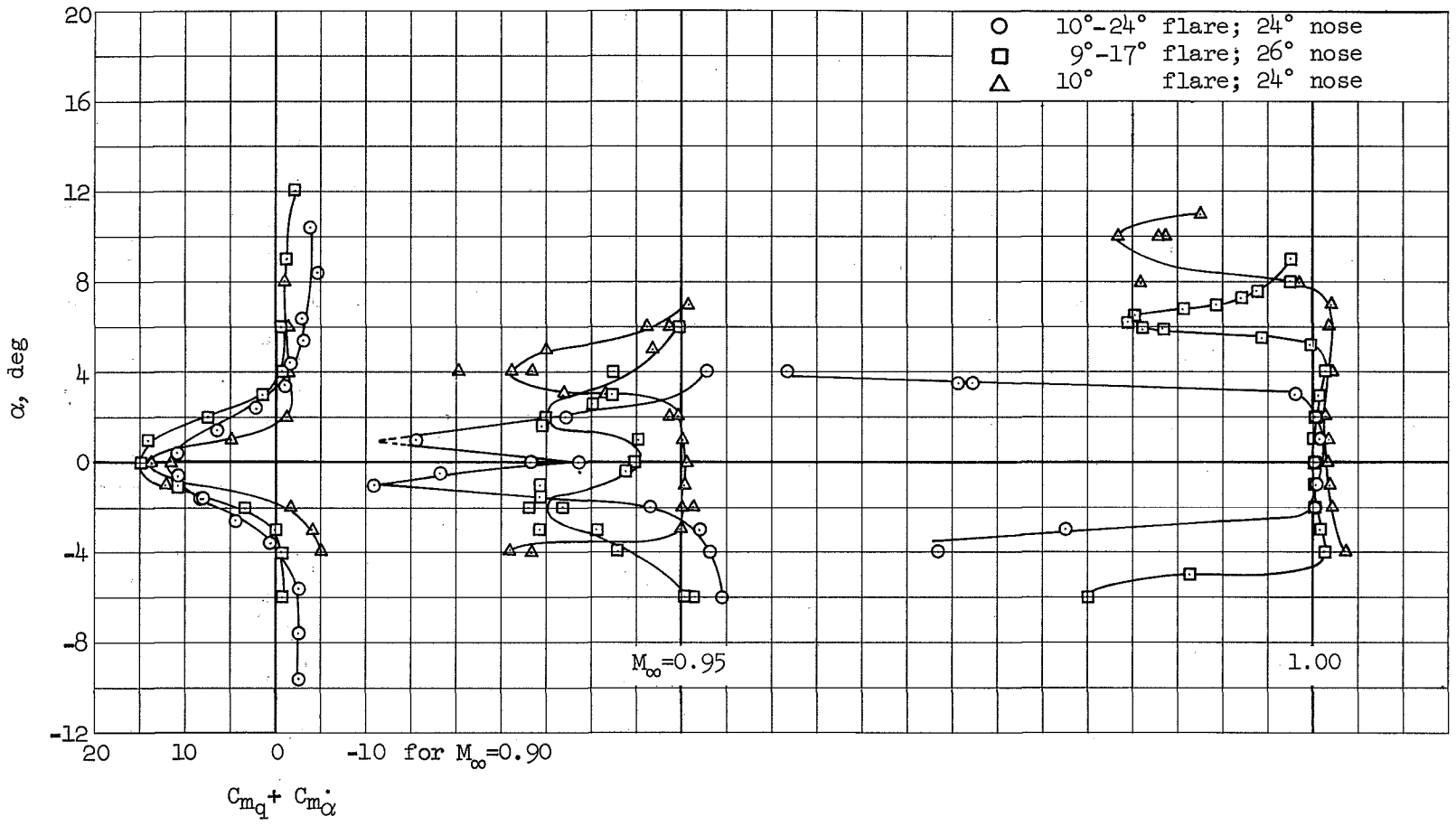

(a) M_∞ = 0.90 to 1.00

Figure 10.- Variation of the damping in pitch with angle of attack at constant Mach number for blunt-nosed models.

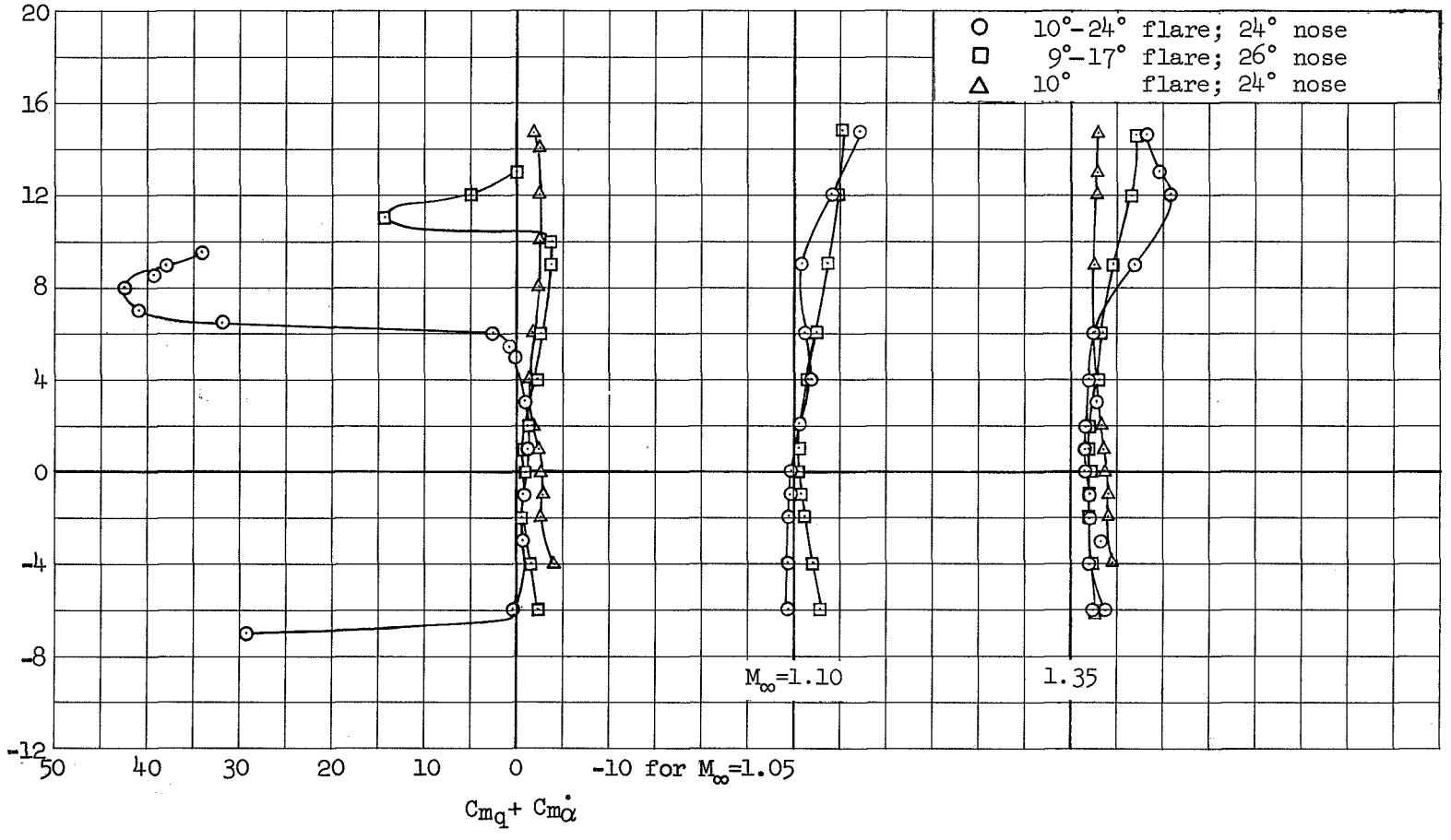

(b) M_∞ = 1.05 to 1.35

Figure 10.- Concluded.

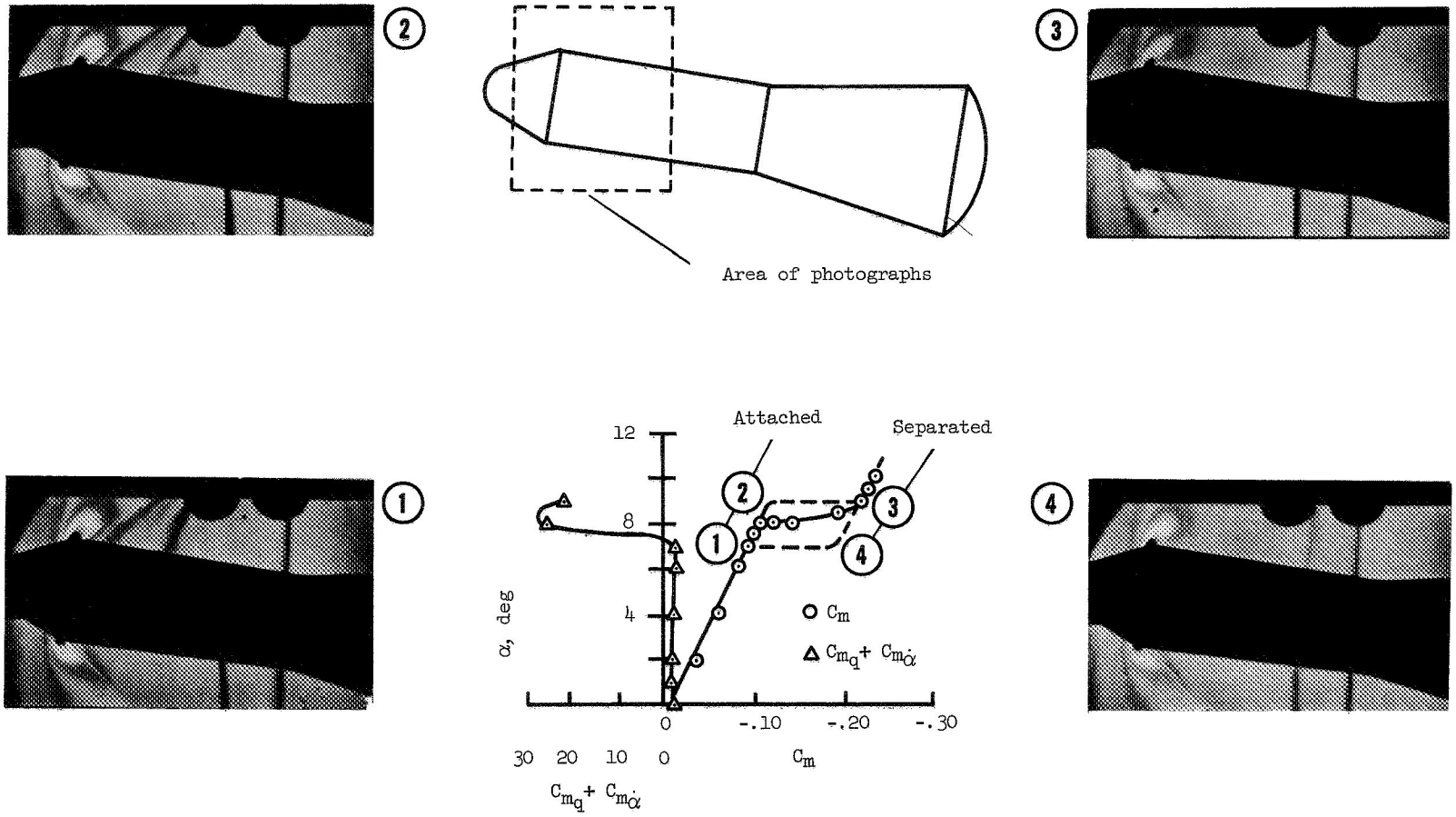

$M_\infty = 1.00$

Figure 11.- Schlieren motion pictures of attached and separated flow conditions during pitch oscillations.

NASA-Langley, 1962 A-525

DECLASSIFIED